COLLECTIVE PROPERTIES OF "DEFORMED" SUPERHEAVY NUCLEI*

I. MUNTIAN[a,b] AND A. SOBICZEWSKI[a]

[a]A. Soltan Institute for Nuclear Studies
Hoża 69, 00-681 Warsaw, Poland
[b]Institute for Nuclear Research, Kiev, Ukraine

(Received December 22, 2000)

Problem of production of even–even superheavy nuclei in their first excited state 2+ is discussed. Measurement of energy of this state is considered as a way to learn if these nuclei are deformed. Superheavy nuclei situated around the nucleus ^{270}Hs, which according to calculations are expected to be deformed, are studied. Particular attention is given to calculations of the branching ratio p_{2+}/p_{0+} between α decay of a nucleus to the 2+ state and to the ground state 0+ of its daughter. Sensitivity of this ratio to various factors appearing in the calculations is discussed.

PACS numbers: 21.10.Re, 21.60.Ev, 27.90.+b

1. Introduction

The heaviest nuclei, for which collective states have been observed, are ^{254}No [1,2] and ^{252}No [3]. These are the states of the ground-state rotational bands studied by the in-beam γ spectroscopy. There is a little chance, however, to extend these studies to superheavy nuclei, in the nearest future. This is because of very low cross section for synthesis of these nuclei and, simultaneously, of a relatively low effectiveness of γ spectroscopy. A larger chance is to observe the first excited 2+ state of an even–even superheavy nucleus in α-decay or electron spectra. The observation of this state would solve the important problem of shapes of these nuclei: are they deformed or not. If the energy of the state is very low, about 40–50 keV, as predicted in calculations [4–6], the state is of the rotational nature and, thus, the nuclei are deformed. Such result would be in line with many theoretical calculations of shapes of these nuclei (*e.g.* Refs. [7–16]).

* Presented at the XXXV Zakopane School of Physics "Trends in Nuclear Physics", Zakopane, Poland, September 5–13, 2000.

The importance of solution of this problem is that it would show experimentally that large shell effects, needed [17] for existence of these already observed nuclei, also appear in deformed nuclei, and not only in spherical ones, as was thought for a long time.

To estimate the chance to observe the lowest $2+$ state in the discussed nuclei, the ratio of the probability of α decay to this state, p_{2+}, to that to the ground-state $0+$, p_{0+}, has been calculated in Refs. [5,6]. Coulomb and centrifugal interactions between α particle and a daughter nucleus have been taken into account when calculating the potential-energy barrier penetrated by α particle.

The objective of this paper is to extend the discussion of the ratio p_{2+}/p_{0+}. The influence of inclusion of a nuclear interaction, of the proximity type [18], to the barrier is considered.

Method of the calculations is described in Sect. 2 and the results are given in Sect. 3. Section 4 presents a discussion of various factors influencing the ratio p_{2+}/p_{0+}.

2. Method of the calculations

The ground-state energy of a nucleus is calculated in a macroscopic–microscopic approach. The Yukawa-plus-exponential model [19] is taken for the macroscopic part of the energy and the Strutinski shell correction, based on the Woods–Saxon single-particle potential [20], is used for the microscopic part.

Equilibrium deformation of a nucleus is obtained by minimization of its energy in a multidimensional deformation space [21]. The 7-dimensional space $\{\beta_\lambda\}$, $\lambda = 2, 3, ..., 8$, is taken.

Moment of inertia of a nucleus is calculated in the cranking approximation [22]. It has been shown in a number of papers (*e.g.* Refs. [23–25]) that this approach allows for a good description of the ground-state moments of inertia of well deformed nuclei, especially of heavy ones [25].

To estimate the probability of α decay of a nucleus to the first rotational state $2+$ of its daughter, p_{2+}, it is sufficient to calculate the ratio p_{2+}/p_{0+}. This is because the probability (more exactly the half-life) of the decay to the ground state $0+$ has been already calculated for superheavy nuclei in a number of papers (*e.g.* Refs. [12,14,16,26]) and also measured for some of these nuclei (*cf. e.g.* Refs. [27–29]).

The probability p_{I+} is usually considered as

$$p_{I+} = w_{I+} \cdot P_{I+} \,, \tag{2.1}$$

where w_{I+} is the reduced decay probability and P_{I+} is the probability to penetrate the potential-energy barrier by α particle with angular momen-

tum I. One should mention that the probability p_{I+} has been studied for already a long time (*e.g.* Refs. [30]). According to Eq. (2.1), the ratio of p_{2+}/p_{0+} is

$$\frac{p_{2+}}{p_{0+}} = \frac{w_{2+}}{w_{0+}} \frac{P_{2+}}{P_{0+}} \,. \tag{2.2}$$

The penetration probability P_{I+} is calculated in the quasiclassical WKB approximation

$$P_{I+}\,(Z,N) = \exp\left\{ -\frac{2}{\hbar}\sqrt{2m_\alpha} \int\limits_{r_{\rm en}}^{r_{\rm ex}} [V\,(r) - E]^{1/2}\, dr \right\}, \tag{2.3}$$

where $V(r)$ is the potential energy considered as a function of the distance r between the centers of the α particle and the nucleus, and E is the decay energy of the parent nucleus to the state $I+$ of the considered nucleus (Z,N), *i.e.*

$$E(Z,N) = Q_\alpha(Z+2, N+2) - E_{I+}(Z,N) \equiv Q_{\alpha{\rm p}} - E_{I+}\,, \tag{2.4}$$

where E_{I+} is the rotational energy of the $I+$ state of a nucleus (Z,N) and $Q_{\alpha{\rm p}}$ is the α-decay energy of the parent nucleus. In Eq. (2.3), m_α is reduced mass of α particle, $r_{\rm en}$ is the value of r at the entrance point of α particle to the barrier and $r_{\rm ex}$ is the value of r at the exit point from the barrier.

The potential energy is considered in two variants. One is when only Coulomb and centrifugal energies are contributing to the barrier

$$V(r) = \frac{2Ze^2}{r} + \frac{\hbar^2 I(I+1)}{2m_\alpha r^2} \,. \tag{2.5}$$

The second variant is, when a nuclear interaction is also included

$$V(r) = \frac{2Ze^2}{r} + \frac{\hbar^2 I(I+1)}{2m_\alpha r^2} + V_{\rm nucl}(r) \,. \tag{2.6}$$

The potential energy $V(r)$ is considered in the region of the contact and outside of the contact configuration of α particle and a daughter nucleus, *i.e.* for $r \geq C + C_\alpha$, where C and C_α are half-density radii of a daughter nucleus and α particle, respectively.

For the nuclear potential $V_{\rm nucl}$, we take the proximity interaction of Ref. [18]. Let us remind its details. The potential is

$$V_{\rm p} = K\Phi(\zeta)\,, \tag{2.7}$$

where $K = 4\pi\gamma b\bar{C}$ with $\bar{C} = CC_\alpha/(C+C_\alpha)$. Density radius C of a nucleus (also for α particle) is related to its effective (sharp surface) radius R by

$$C \approx R - \frac{b^2}{R}\,, \tag{2.8}$$

where b is the surface diffuseness of a nucleus, assumed as $b = 1$ fm. The effective radius is taken as

$$R = (1.28A^{1/3} - 0.76 + 0.8A^{-1/3}) \ \text{fm} \tag{2.9}$$

and the nuclear-surface tension parameter γ as

$$\gamma = 0.9517(1 - 1.7826I^2) \ \text{MeV/fm}^2, \tag{2.10}$$

where $I = (N-Z)/A$ is the relative neutron excess.

The function $\Phi(\zeta)$ is

$$\begin{aligned} \Phi(\zeta) \ &\approx \ -1.7817 + 0.9270\zeta + 0.01696\zeta^2 - 0.05148\zeta^3\,, \\ &\quad \text{for} \ \ 0 \le \zeta \le 1.9475, \end{aligned} \tag{2.11}$$

$$\begin{aligned} \Phi(\zeta) \ &\approx \ -4.41 \exp\frac{-\zeta}{0.7176}\,, \\ &\quad \text{for} \ \ \zeta \ge 1.9475\,, \end{aligned} \tag{2.12}$$

where $\zeta = [r - (C + C_\alpha)]/b$.

The ratio of reduced probabilities w_{2+}/w_{0+} is treated phenomenologically. We find that, similarly as in Refs. [5,6], the ratio may be well described by a 2-parameter formula

$$\frac{w_{2+}}{w_{0+}} = 10^{(aA+b)} \tag{2.13}$$

and, thus, the ratio of the total probabilities is

$$\frac{p_{2+}}{p_{0+}} = 10^{(aA+b)}\frac{P_{2+}}{P_{0+}}\,, \tag{2.14}$$

where A is the mass number of a nucleus.

Adjustment of the parameters a and b to experimental results for p_{2+}/p_{0+}, obtained for 26 nuclei [31], with P_{2+}/P_{0+} calculated with the use of Eq. (2.3), leads to the following values

$$a = -0.02685, \qquad b = 6.3659\,, \tag{2.15}$$

and reproduces the experimental values of p_{2+}/p_{0+} with rms deviations equal to 0.027, in the case when only Coulomb and centrifugal terms, Eq. (2.5),

contribute to the barrier. In the case, when also the nuclear proximity potential is included, the corresponding results are very similar

$$a = -0.02692\,, \qquad b = 6.3963\,, \tag{2.16}$$

with rms deviation also equal to 0.027.

Thus, we find that the inclusion of nuclear interaction to the barrier does not practically change the quality of description of experimental values for p_{2+}/p_{0+}. We also find that the differences between nuclear radii taken in this paper and in Refs. [5,6] do not practically influence this description either.

3. Results

To illustrate the results obtained in the calculations of the equilibrium shapes of analized nuclei, we show these shapes in Fig. 1. They have been calculated for a large region of nuclei with proton number Z=82–130 and neutron number N=126–190. One can see that most of the nuclei are deformed, in particular those around ^{270}Hs.

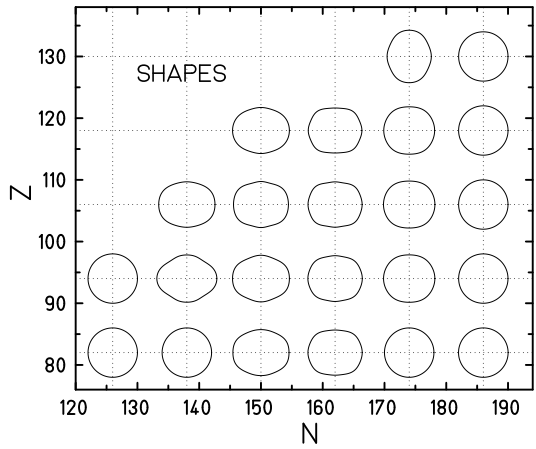

Fig. 1. Shapes of nuclei plotted for a wide region of Z=82–130 and N=126–190.

To see how well established is the deformation, the deformation energy $E_{\rm def}$ (*i.e.* the gain in energy of a nucleus due to its deformation) calculated for these nuclei is given in Fig. 2. The analysis of this quantity in various nuclei [23] indicates that nuclei with $E_{\rm def} \gtrsim 2$ MeV are well deformed, while those with $E_{\rm def} < 2$ MeV are rather transitional or spherical. One can see in Fig. 2 that most of the considered nuclei are well deformed. The largest values of $E_{\rm def}$ (above 12 MeV) are obtained for nuclei around the nucleus ^{254}No, *i.e.* for nuclei with the largest quadrupole deformation β_2^0.

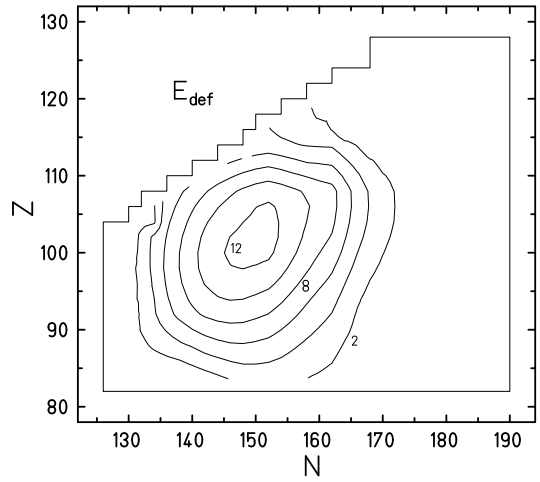

Fig. 2. Contour map of the deformation energy $E_{\rm def}$.

Figure 3 illustrates the rotational energy E_{2+} calculated for heaviest nuclei (with $Z > 100$). The figure is taken from Ref. [6]. One can see that the energy is very low, around 40–50 keV. This is because the nuclei are well deformed and also very heavy. Shell effects at neutron numbers N=152 and 162 are clearly seen in the dependence of this energy on N.

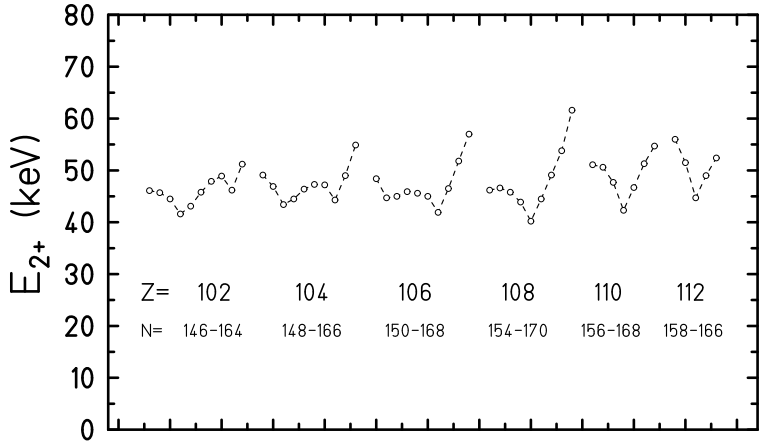

Fig. 3. Dependence of the energy E_{2+} on neutron number N, calculated for elements with proton number Z=102–112. For each element, values of considered N are specified below the value of Z.

Description of the experimental values of p_{2+}/p_{0+} by calculations in the case of the barrier without proximity forces is illustrated in Fig. 4. As mentioned in Sect. 2, the values of p_{2+}/p_{0+} calculated in this paper are practically the same as those obtained in Ref. [6], although values of nuclear radii assumed in these two papers, differ from each other. Thus, Fig. 4 is practically the same as the corresponding figure in Ref. [6]. Also the values of p_{2+}/p_{0+} calculated with inclusion of nuclear proximity interaction to the barrier are practically the same as those obtained without this interaction. Due to this, we do not show these values in Fig. 4, as they would not be distinguishable from those obtained without this interaction.

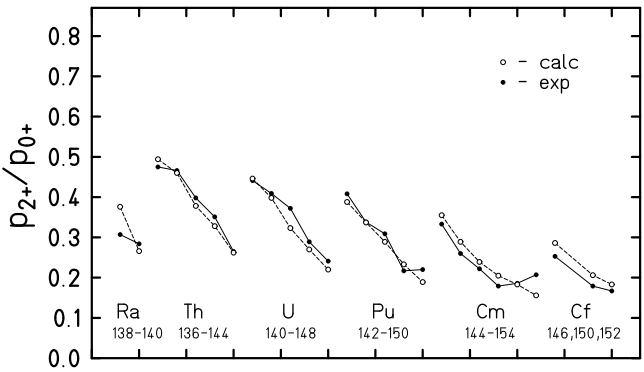

Fig. 4. Comparison between calculated and experimental values of the branching ratio p_{2+}/p_{0+} for nuclei of the elements: Ra-Cf, with neutron number N specified below the symbol of each element.

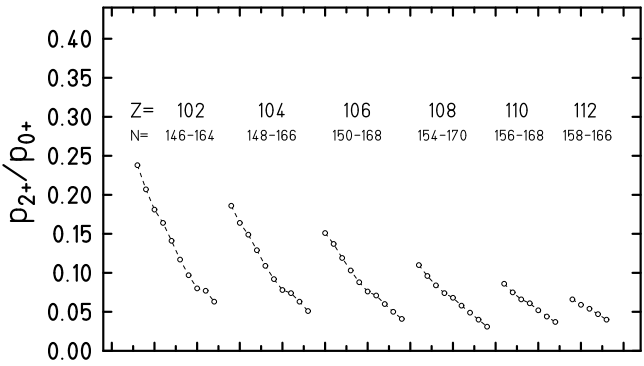

Fig. 5. Same as in Fig. 3, but for the branching ratio p_{2+}/p_{0+}.

Values of p_{2+}/p_{0+} calculated for transfermium nuclei with Z=102–112 in the case without proximity interaction are shown in Fig. 5. The values calculated with inclusion of proximity forces are very close to them and they are not shown in Fig. 5, similarly as it was in the case of lighter nuclei discussed in Fig. 4. The effect of the inclusion of the proximity forces on the ratio p_{2+}/p_{0+} is discussed in more details in the next section.

4. Discussion of various effects

It is interesting to see the role of various factors in the results for the branching ratio p_{2+}/p_{0+}.

4.1. Contribution of various interactions to the barrier

Figure 6 illustrates contribution of the Coulomb, nuclear (proximity) and centrifugal interactions to the barrier penetrated by α particle. The figure is plotted for ^{238}U. One can see that the Coulomb interaction is most important. The proximity force is significant only at the beginning of the barrier and the centrifugal force is generally very small in the barrier region for such a heavy (large) nucleus as ^{238}U. The entrance point to the barrier, $r_{\rm en}$, and the exit point from it, $r_{\rm ex}$, are indicated.

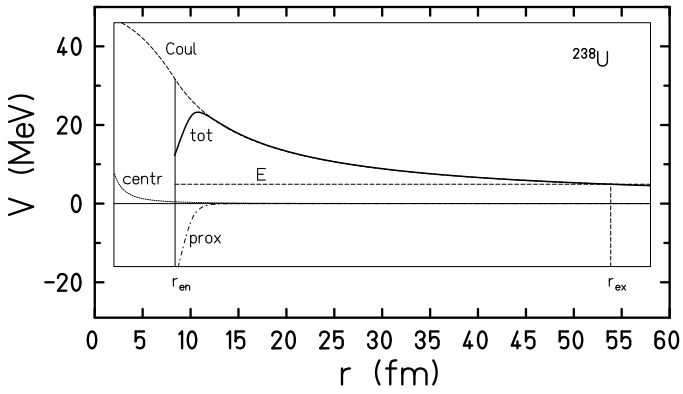

Fig. 6. Potential-energy barrier for α particle as a function of the distance r between centres of α particle and a daughter nucleus. The total barrier (tot) is composed of the Coulomb (Coul), proximity (prox) and centrifugal (centr) contributions to it.

4.2. Role of the energy E_{2+}

The energy of the first excited state 2+, E_{2+}, influences (decreases) the penetration probability P_{2+} (*cf.* Eqs. (2.3) and (2.4)) and, thus, the ratio P_{2+}/P_{0+}. Although this energy is small, about 40–50 keV, the influence is

significant. This is directly illustrated in Fig. 7, where values of P_{2+}/P_{0+} are calculated with inclusion of E_{2+} and without it, for the same nuclei as in Fig. 4. One can see that the inclusion of E_{2+} decreases this ratio by a factor of: from about 4 for the lightest to about 1.5 for the heaviest of the nuclei considered in Fig. 7. The barrier is calculated with the inclusion of the proximity interaction. The entrance point to it, $r_{\rm en}$, is obtained with the use of Eqs. (2.8) and (2.9).

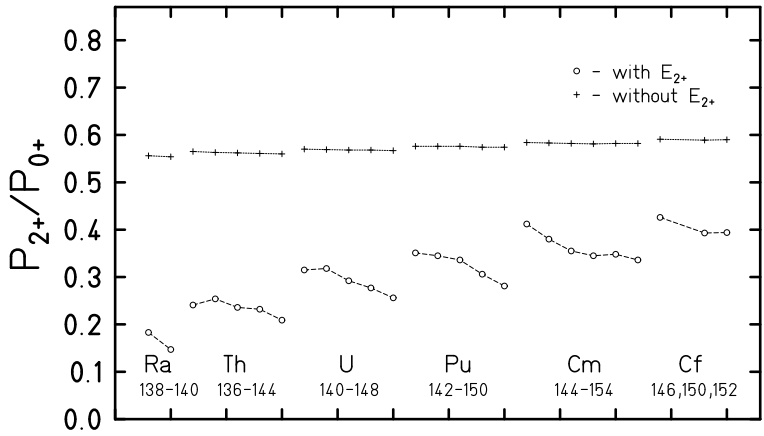

Fig. 7. Same as in Fig. 4, but for the ratio P_{2+}/P_{0+} calculated in two variants: with inclusion of the energy E_{2+} and without it.

4.3. Role of the reduced probability

To see the role of the ratio of the reduced probabilities w_{2+}/w_{0+} in reproducing the ratio of the experimental values of the total probabilities p_{2+}/p_{0+}, let us compare the latter with calculated values of P_{2+}/P_{0+}. This is done in Fig. 8. One can see that the isotopic dependences, and generally the dependences on the mass number A, of the two quantities are very different. Experimental values of p_{2+}/p_{0+} are fast decreasing, while calculated values of P_{2+}/P_{0+} are increasing, with increasing A. Thus, according to Eq. (2.2), the role of w_{2+}/w_{0+}, which is treated phenomenologically, is to make the theoretical ratio p_{2+}/p_{0+} a decreasing function of A as the experimental one is. The result, calculated according to Eqs. (2.13) and (2.16) is shown in Fig. 9. One can see that it is really a function, which is fast decreasing with increasing mass number A.

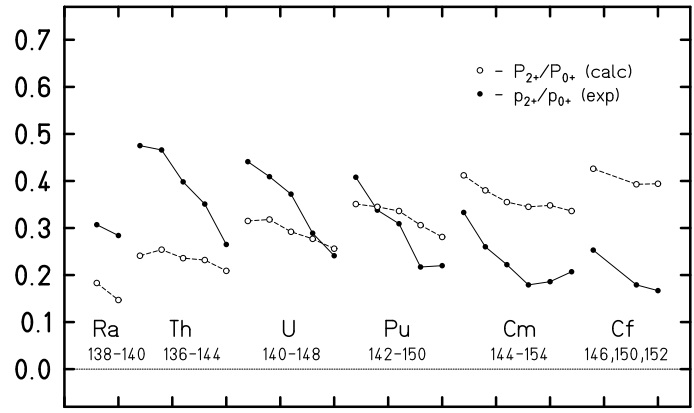

Fig. 8. Same as in Fig. 4, but for the calculated values of P_{2+}/P_{0+} and experimental values of p_{2+}/p_{0+}.

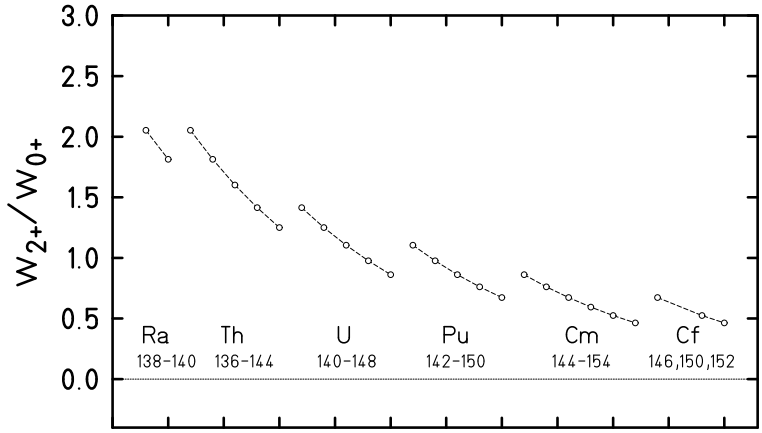

Fig. 9. Same as in Fig. 4, but for the calculated values of the ratio w_{2+}/w_{0+}.

4.4. Role of various factors in heaviest nuclei

In this subsection, we will illustrate the role of various factors influencing the ratio p_{2+}/p_{0+} calculated for the heaviest nuclei with Z=102–112.

The results are given in Table I. The first 3 columns specify proton, neutron and mass numbers of a nucleus. Columns 4 and 5 give calculated energy of the first 2+ state of a nucleus and the α-decay energy of its parent, respectively.

TABLE I

Energies E_{2+} and $Q_\alpha^{\rm par}$, few variants of the ratio P_{2+}/P_{0+} and the ratio w_{2+}/w_{0+} calculated for nuclei with proton number $Z = 102 - 112$ (see text).

Z	N	A	$E_{2+}^{\rm th}$	$Q_\alpha^{\rm par}$	$\frac{P_{2+}}{P_{0+}}$	$\frac{P_{2+}}{P_{0+}}$	$\frac{P_{2+}}{P_{0+}}$	$\frac{P_{2+}}{P_{0+}}$	$\frac{w_{2+}}{w_{0+}}$	$\frac{p_{2+}}{p_{0+}}$
—	—	—	keV	MeV	—	—	—	—	—	%
1	2	3	4	5	6	7	8	9	10	11
102	146	248	46.1	9.85	0.634	0.480	0.475	0.454	0.525	23.9
102	148	250	45.7	9.43	0.632	0.470	0.465	0.446	0.464	20.7
102	150	252	44.5	9.10	0.631	0.465	0.460	0.442	0.410	18.1
102	152	254	41.6	9.20	0.632	0.477	0.472	0.454	0.362	16.4
102	154	256	43.1	8.84	0.630	0.462	0.457	0.440	0.320	14.1
102	156	258	45.8	8.26	0.627	0.435	0.430	0.415	0.282	11.7
102	158	260	47.9	7.70	0.624	0.407	0.402	0.389	0.250	9.7
102	160	262	48.9	7.15	0.622	0.380	0.376	0.364	0.220	8.0
102	162	264	46.2	7.64	0.626	0.411	0.407	0.393	0.195	7.7
102	164	266	51.2	7.40	0.624	0.383	0.379	0.367	0.172	6.3
104	148	252	49.1	10.19	0.639	0.480	0.475	0.454	0.410	18.6
104	150	254	46.9	9.90	0.638	0.479	0.474	0.454	0.362	16.5
104	152	256	43.4	9.96	0.639	0.491	0.486	0.466	0.320	14.9
104	154	258	44.5	9.60	0.637	0.479	0.473	0.455	0.282	12.9
104	156	260	46.4	9.06	0.634	0.457	0.452	0.436	0.250	10.9
104	158	262	47.3	8.54	0.632	0.438	0.433	0.418	0.220	9.2
104	160	264	47.2	8.05	0.629	0.421	0.417	0.403	0.195	7.9
104	162	266	44.3	8.66	0.634	0.453	0.448	0.433	0.172	7.5
104	164	268	49.0	8.46	0.633	0.430	0.426	0.411	0.152	6.3
104	166	270	54.9	8.11	0.631	0.398	0.393	0.380	0.134	5.1
106	150	256	48.4	10.97	0.646	0.501	0.495	0.473	0.320	15.1
106	152	258	44.7	11.02	0.647	0.512	0.506	0.484	0.282	13.7
106	154	260	45.0	10.69	0.646	0.504	0.499	0.477	0.250	11.9
106	156	262	45.9	10.20	0.643	0.490	0.484	0.465	0.220	10.3
106	158	264	45.6	9.65	0.641	0.476	0.471	0.453	0.195	8.8
106	160	266	45.0	9.13	0.638	0.464	0.458	0.442	0.172	7.6
106	162	268	41.9	9.79	0.642	0.492	0.485	0.469	0.152	7.1
106	164	270	46.5	9.58	0.642	0.473	0.467	0.450	0.134	6.1
106	166	272	51.8	9.22	0.640	0.446	0.441	0.425	0.119	5.1
106	168	274	57.0	8.77	0.638	0.414	0.409	0.395	0.105	4.2

TABLE I cont.

Z	N	A	$E_{2+}^{\rm th}$	$Q_\alpha^{\rm par}$	$\frac{P_{2+}}{P_{0+}}$	$\frac{P_{2+}}{P_{0+}}$	$\frac{P_{2+}}{P_{0+}}$	$\frac{P_{2+}}{P_{0+}}$	$\frac{w_{2+}}{w_{0+}}$	$\frac{p_{2+}}{p_{0+}}$
—	—	—	keV	MeV	—	—	—	—	—	%
1	2	3	4	5	6	7	8	9	10	11
108	154	262	46.2	12.17	0.656	0.533	0.526	0.501	0.220	11.1
108	156	264	46.6	11.76	0.655	0.523	0.517	0.494	0.195	9.6
108	158	266	45.8	11.24	0.652	0.515	0.509	0.487	0.172	8.4
108	160	268	43.9	10.80	0.650	0.510	0.504	0.484	0.152	7.4
108	162	270	40.2	11.39	0.654	0.534	0.528	0.505	0.134	6.8
108	164	272	44.5	11.03	0.652	0.515	0.509	0.488	0.119	5.8
108	166	274	49.1	10.52	0.650	0.490	0.484	0.465	0.105	4.9
108	168	276	53.8	9.84	0.646	0.457	0.452	0.436	0.093	4.0
108	170	278	61.6	8.86	0.641	0.401	0.397	0.384	0.082	3.1
110	156	266	51.1	12.59	0.661	0.529	0.523	0.497	0.172	8.6
110	158	268	50.6	12.07	0.659	0.520	0.514	0.490	0.152	7.5
110	160	270	47.7	11.67	0.657	0.519	0.513	0.491	0.134	6.6
110	162	272	42.3	12.13	0.660	0.542	0.536	0.512	0.119	6.1
110	164	274	46.7	11.83	0.659	0.525	0.519	0.497	0.105	5.2
110	166	276	51.3	11.36	0.657	0.503	0.498	0.477	0.093	4.4
110	168	278	54.7	10.65	0.653	0.476	0.471	0.453	0.082	3.7
112	158	270	56.0	12.76	0.664	0.520	0.514	0.490	0.134	6.6
112	160	272	51.5	12.41	0.663	0.524	0.518	0.495	0.119	5.9
112	162	274	44.7	12.75	0.665	0.548	0.541	0.517	0.105	5.4
112	164	276	49.0	12.54	0.665	0.534	0.528	0.504	0.093	4.7
112	166	278	52.4	12.13	0.663	0.517	0.511	0.489	0.082	4.0

Columns 6 and 7 present values of P_{2+}/P_{0+} calculated without and with the energy E_{2+}, respectively, included in the integrand appearing in Eq. (2.3). Thus, they illustrate the role of E_{2+} in P_{2+}/P_{0+}, similarly as was done in Fig. 7 for lighter nuclei. One can see that the inclusion of E_{2+} reduces P_{2+}/P_{0+} by a factor of about 1.3–1.6 for the nuclei considered in the Table. Here, the ratio P_{2+}/P_{0+} is calculated with the total effective radii $R = 1.40A^{1/3}$ fm and without the proximity forces, *i.e.* in the same way as in Refs. [5,6]. The total effective radius may be understood as the radius of the daughter nucleus with a sharp surface, while α particle is a point nucleus. Then the distance between centres of the two nuclei in the touching configuration corresponding to the entrance point to the barrier is: $r_{\rm en} = R$.

Column 8 gives values P_{2+}/P_{0+} calculated with nuclear radii adopted in the present paper, Eqs. (2.8) and (2.9), and without proximity forces. Thus, a comparison between the values of the columns 7 and 8 shows the

effect of a change of nuclear radii on P_{2+}/P_{0+}. Let us note that the entrance point to the barrier, $r_{\rm en}$, appears earlier in the case of column 8, *i.e.* in the case of diffuse nuclear surfaces, than in the case of column 7. For example, $r_{\rm en} = C + C_\alpha = 8.38$ fm in the case of column 8, while $r_{\rm en} = 1.40(238)^{1/3} = 8.68$ fm in the case of column 7, for the nucleus ^{238}U. Thus, a part of the barrier is added in the case of column 8, where a relatively large centrifugal interaction is present, which hinders the decay to the 2+ state. As a result, the ratio P_{2+}/P_{0+} should be reduced in this case. One can see in Table I that really this ratio is reduced in column 8 with respect to that of column 7 by a factor of about 0.94–0.96, *i.e.* by about 6–4 %.

Column 9 presents values of P_{2+}/P_{0+} calculated in the same way as those of column 8, but with inclusion of the proximity forces. Thus, a comparison between them and the values of column 8 gives the effect of the proximity forces on the ratio P_{2+}/P_{0+}. One can see that this effect is small. The inclusion of the proximity interaction in the barrier results in smaller, but only by about 3–4 % values of P_{2+}/P_{0+}.

The proximity forces strongly change the barrier for α particle, as is shown in Fig. 6, and, this way, also each of the probabilities P_{2+} and P_{0+}. The ratio of them, however, remains almost unchanged. This results in a small effect of the proximity forces on the ratio w_{2+}/w_{0+} of the reduced probabilities, as it is adjusted to the calculated P_{2+}/P_{0+} to reproduce experimental values of the ratio p_{2+}/p_{0+} of the total probabilities. As a consequence, the effect of the proximity forces on the calculated values of p_{2+}/p_{0+} is also small, about the same as on the ratio P_{2+}/P_{0+}, *i.e.* of about 3–4 %.

Values of the ratio w_{2+}/w_{0+}, calculated according to Eqs. (2.13) and (2.16), are given in column 10. One can see that they fast decrease with increasing mass number A, similar as in Fig. 3, where they were calculated in the same way, but only for lighter nuclei. The ratio decreases from 0.52, for the lightest, to 0.08 for the heaviest, nuclei considered in the table.

In conclusion, one can say that the probabilities of the penetration of the potential-energy barrier by α particle in the first excited state 2+ and in the ground-state 0+ of an even–even heavy nucleus, P_{2+} and P_{0+}, strongly depend on such factors as radius of a nucleus or the shape of the barrier (depending *e.g.* on whether nuclear forces of the proximity type is included to it or not). The ratio, however, of these quantities, P_{2+}/P_{0+}, is rather insensitive to these factors.

The authors would like to thank S. Hofmann, T.L. Khoo, M. Leino, Z. Patyk and W.J. Świątecki for helpful discussions. Support by the Polish State Committee for Scientific Research (KBN), Grant No. 2 P03B 117 15, and by the Bogoliubov–Infeld Programme is gratefully acknowledged.

REFERENCES

[1] P. Reiter *et al.*, *Phys. Rev. Lett.* **82**, 509 (1999).

[2] M. Leino *et al.*, *Eur. Phys. J.* **A6**, 63 (1999).

[3] R.-D. Herzberg, M. Leino, private communication.

[4] I. Muntian, Z. Patyk, A. Sobiczewski, *Acta Phys. Pol.* **B30**, 689 (1999); *Phys. Rev.* **C60**, 041 302 (1999).

[5] I. Muntian, Z. Patyk, A. Sobiczewski, *Phys. Lett.*, to be published (2001).

[6] A. Sobiczewski, I. Muntian, Z. Patyk, *Phys. Rev.* **C63**, (2001), in press.

[7] S. Ćwiok, V.V. Pashkevich, J. Dudek, W. Nazarewicz, *Nucl. Phys.* **A410**, 254 (1983).

[8] P. Möller, G.A. Leander, J.R. Nix, *Z. Phys.* **A323**, 41 (1986).

[9] K. Böning, Z. Patyk, A. Sobiczewski, S. Ćwiok, *Z. Phys.* **A325**, 479 (1986).

[10] A. Sobiczewski, Z. Patyk, S. Ćwiok, *Phys. Lett.* **B186**, 6 (1987).

[11] Z. Patyk, J. Skalski, A. Sobiczewski, S. Ćwiok, *Nucl. Phys.* **A502**, 591c (1989).

[12] Z. Patyk, A. Sobiczewski, *Nucl. Phys.* **A533**, 132 (1991).

[13] P. Möller, J.R. Nix, W.D. Myers, W.J. Świątecki, *At. Data Nucl. Data Tables* **59**, 185 (1995).

[14] J.-F. Berger, J. Bitaud, J. Decharge, M. Girod, S. Peru-Desenfants, in Proceedings of the 24th International Workshop "Extremes of Nuclear Stucture", Hirschegg (Austria) 1996, edited by H. Feldmeier, J. Knoll and W. Nörenberg, GSI, Darmstadt 1996, p. 43.

[15] G.A. Lalazissis, M.M. Sharma, P. Ring, Y.K. Gambhir, *Nucl. Phys.* **A608**, 202 (1996).

[16] R.R. Chasman, I. Ahmad, *Phys. Lett.* **B392**, 255 (1997).

[17] Z. Patyk, A. Sobiczewski, P. Armbruster, K.-H. Schmidt, *Nucl. Phys.* **A491**, 267 (1989).

[18] Yi-Jin Shi, W.J. Świątecki, *Phys. Rev. Lett.* **54**, 300 (1985).

[19] H.J. Krappe, J.R. Nix, A.J. Sierk, *Phys. Rev.* **C20**, 992 (1979).

[20] S. Ćwiok, J. Dudek, W. Nazarewicz, J. Skalski, T. Werner, *Comput. Phys. Commun.* **46**, 379 (1987).

[21] A. Sobiczewski, Z. Patyk, S. Ćwiok, P. Rozmej, *Nucl. Phys.* **A485**, 16 (1988).

[22] D.R. Inglis, *Phys. Rev.* **96**, 1059 (1954).

[23] I. Ragnarsson, A. Sobiczewski, R.K. Sheline, S.E. Larsson, B. Nerlo-Pomorska, *Nucl. Phys.* **A233**, 329 (1974).

[24] I. Hamamoto, *Phys. Lett.* **B56**, 431 (1975).

[25] K. Pomorski, A. Sobiczewski, *Acta Phys. Pol.* **B9**, 61 (1978).

[26] R. Smolańczuk, A. Sobiczewski, in Proceedings of the XV Nuclear Physics Conference "Low Energy Nuclear Dynamics", St. Petersburg (Russia) 1995, edited by Yu.Ts. Oganessian, W. von Oertzen and R. Kalpakchieva, World Scientific, Singapore 1995, p. 313.

[27] S. Hofmann, *Rep. Prog. Phys.* **61**, 639 (1998); *Acta Phys. Pol.* **B30**, 621 (1999).

[28] Yu.Ts. Oganessian, in *Heavy Elements and Related New Phenomena*, edited by W. Greiner and R.K. Gupta, World Scientific, Singapore 1999, vol. 1, chap. 2.

[29] S. Hofmann, G. Münzenberg, *Rev. Mod. Phys.* **72**, (2000).

[30] J.O. Rasmussen, *Phys. Rev.* **113**, 1593 (1959); **115**, 1675 (1959).

[31] *Table of Isotopes*, 8th edition, edited by R.B. Firestone and V.S. Shirley, J. Wiley, New York 1996, vol. 2.